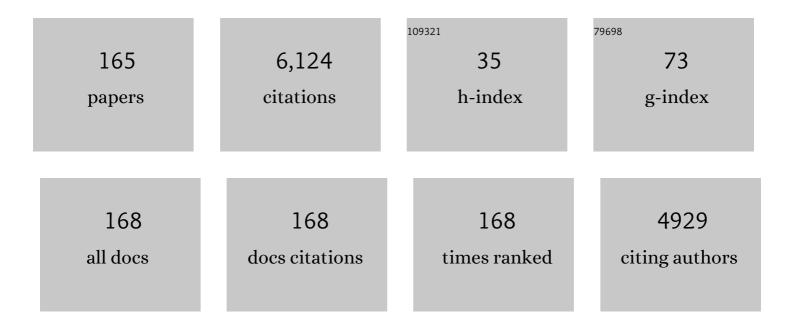
Marinko V Sarunic

List of Publications by Year in descending order

Source: https://exaly.com/author-pdf/5094290/publications.pdf Version: 2024-02-01



#	Article	IF	CITATIONS
1	Sensitivity advantage of swept source and Fourier domain optical coherence tomography. Optics Express, 2003, 11, 2183.	3.4	1,888
2	Instantaneous complex conjugate resolved spectral domain and swept-source OCT using 3x3 fiber couplers. Optics Express, 2005, 13, 957.	3.4	174
3	Quantitative Optical Coherence Tomography Angiography of Radial Peripapillary Capillaries in Glaucoma, Glaucoma Suspect, and Normal Eyes. American Journal of Ophthalmology, 2016, 170, 41-49.	3.3	165
4	RETOUCH: The Retinal OCT Fluid Detection and Segmentation Benchmark and Challenge. IEEE Transactions on Medical Imaging, 2019, 38, 1858-1874.	8.9	139
5	Segmentation of Intra-Retinal Layers From Optical Coherence Tomography Images Using an Active Contour Approach. IEEE Transactions on Medical Imaging, 2011, 30, 484-496.	8.9	136
6	Full-field swept-source phase microscopy. Optics Letters, 2006, 31, 1462.	3.3	119
7	Graphics processing unit accelerated optical coherence tomography processing at megahertz axial scan rate and high resolution video rate volumetric rendering. Journal of Biomedical Optics, 2013, 18, 1.	2.6	109
8	Deep-learning based multiclass retinal fluid segmentation and detection in optical coherence tomography images using a fully convolutional neural network. Medical Image Analysis, 2019, 54, 100-110.	11.6	103
9	Chronic and Acute Models of Retinal Neurodegeneration TrkA Activity Are Neuroprotective whereas p75NTR Activity Is Neurotoxic through a Paracrine Mechanism. Journal of Biological Chemistry, 2010, 285, 39392-39400.	3.4	98
10	Imaging the Ocular Anterior Segment With Real-Time, Full-Range Fourier-Domain Optical Coherence Tomography. JAMA Ophthalmology, 2008, 126, 537.	2.4	96
11	Detailed Visualization of the Anterior Segment Using Fourier-Domain Optical Coherence Tomography. JAMA Ophthalmology, 2008, 126, 765.	2.4	93
12	Wavefront sensorless adaptive optics optical coherence tomography for in vivo retinal imaging in mice. Biomedical Optics Express, 2014, 5, 547.	2.9	91
13	Retinal capillary perfusion: Spatial and temporal heterogeneity. Progress in Retinal and Eye Research, 2019, 70, 23-54.	15.5	90
14	An Agonistic TrkB mAb Causes Sustained TrkB Activation, Delays RGC Death, and Protects the Retinal Structure in Optic Nerve Axotomy and in Glaucoma. , 2010, 51, 4722.		78
15	Ensemble Deep Learning for Diabetic Retinopathy Detection Using Optical Coherence Tomography Angiography. Translational Vision Science and Technology, 2020, 9, 20.	2.2	76
16	Segmentation of the foveal microvasculature using deep learning networks. Journal of Biomedical Optics, 2016, 21, 075008.	2.6	74
17	Frequency estimation precision in Doppler optical coherence tomography using the Cramer-Rao lower bound. Optics Express, 2005, 13, 410.	3.4	73
18	Handheld forward-imaging needle endoscope for ophthalmic optical coherence tomography inspection. Journal of Biomedical Optics, 2008, 13, 020505.	2.6	73

#	Article	IF	CITATIONS
19	Intra-retinal Layer Segmentation in Optical Coherence Tomography Using an Active Contour Approach. Lecture Notes in Computer Science, 2009, 12, 649-656.	1.3	72
20	Wavefront correction and high-resolution in vivo OCT imaging with an objective integrated multi-actuator adaptive lens. Optics Express, 2015, 23, 21931.	3.4	72
21	Real-time quadrature projection complex conjugate resolved Fourier domain optical coherence tomography. Optics Letters, 2006, 31, 2426.	3.3	69
22	<i>In vivo</i> wide-field multispectral scanning laser ophthalmoscopy–optical coherence tomography mouse retinal imager: longitudinal imaging of ganglion cells, microglia, and Müller glia, and mapping of the mouse retinal and choroidal vasculature. Journal of Biomedical Optics, 2015, 20, 126005.	2.6	64
23	In vivo optical imaging of human retinal capillary networks using speckle variance optical coherence tomography with quantitative clinico-histological correlation. Microvascular Research, 2015, 100, 32-39.	2.5	58
24	p75 ^{NTR} and Its Ligand ProNGF Activate Paracrine Mechanisms Etiological to the Vascular, Inflammatory, and Neurodegenerative Pathologies of Diabetic Retinopathy. Journal of Neuroscience, 2016, 36, 8826-8841.	3.6	58
25	Comparisons Between Histology and Optical Coherence Tomography Angiography of the Periarterial Capillary-Free Zone. American Journal of Ophthalmology, 2018, 189, 55-64.	3.3	58
26	Real-time acquisition and display of flow contrast using speckle variance optical coherence tomography in a graphics processing unit. Journal of Biomedical Optics, 2014, 19, 1.	2.6	57
27	In vivo imaging of human photoreceptor mosaic with wavefront sensorless adaptive optics optical coherence tomography. Biomedical Optics Express, 2015, 6, 580.	2.9	57
28	Quantitative Noninvasive Angiography of the Fovea Centralis Using Speckle Variance Optical Coherence Tomography. , 2015, 56, 5074.		56
29	Label-Free Density Measurements of Radial Peripapillary Capillaries in the Human Retina. PLoS ONE, 2015, 10, e0135151.	2.5	56
30	Adaptive optics optical coherence tomography for <i>in vivo</i> mouse retinal imaging. Journal of Biomedical Optics, 2013, 18, 056007.	2.6	52
31	Wavefront sensorless adaptive optics fluorescence biomicroscope for in vivo retinal imaging in mice. Biomedical Optics Express, 2016, 7, 1.	2.9	51
32	RD3 gene delivery restores guanylate cyclase localization and rescues photoreceptors in the Rd3 mouse model of Leber congenital amaurosis 12. Human Molecular Genetics, 2013, 22, 3894-3905.	2.9	50
33	Rapid Volumetric OCT Image Acquisition Using Compressive Sampling. Optics Express, 2010, 18, 21003.	3.4	49
34	Spectral domain second-harmonic optical coherence tomography. Optics Letters, 2005, 30, 2391.	3.3	48
35	Comparative Analysis of Repeatability of Manual and Automated Choroidal Thickness Measurements in Nonneovascular Age-Related Macular Degeneration. , 2013, 54, 2864.		48
36	Quantitative Comparison of Retinal Capillary Images Derived By Speckle Variance Optical Coherence		47

Tomography With Histology. , 2015, 56, 3989.

3

#	Article	IF	CITATIONS
37	Real-time high-speed volumetric imaging using compressive sampling optical coherence tomography. Biomedical Optics Express, 2011, 2, 2690.	2.9	44
38	Optical mapping of the electrical activity of isolated adult zebrafish hearts: acute effects of temperature. American Journal of Physiology - Regulatory Integrative and Comparative Physiology, 2014, 306, R823-R836.	1.8	43
39	Amyloid Beta Immunoreactivity in the Retinal Ganglion Cell Layer of the Alzheimer's Eye. Frontiers in Neuroscience, 2020, 14, 758.	2.8	42
40	Federated Learning for Microvasculature Segmentation and Diabetic Retinopathy Classification of OCT Data. Ophthalmology Science, 2021, 1, 100069.	2.5	40
41	Lens-based wavefront sensorless adaptive optics swept source OCT. Scientific Reports, 2016, 6, 27620.	3.3	39
42	Real-time retinal layer segmentation of OCT volumes with GPU accelerated inferencing using a compressed, low-latency neural network. Biomedical Optics Express, 2020, 11, 3968.	2.9	36
43	Aortic and Cardiac Structure and Function Using High-Resolution Echocardiography and Optical Coherence Tomography in a Mouse Model of Marfan Syndrome. PLoS ONE, 2016, 11, e0164778.	2.5	36
44	In Vivo Imaging of the Mouse Model of X-Linked Juvenile Retinoschisis with Fourier Domain Optical Coherence Tomography. , 2009, 50, 2989.		35
45	Optic Nerve Head and Peripapillary Morphometrics in Myopic Glaucoma. , 2014, 55, 4378.		35
46	Quantitative comparisons between optical coherence tomography angiography and matched histology in the human eye. Experimental Eye Research, 2018, 170, 13-19.	2.6	35
47	Retinal angiography with real-time speckle variance optical coherence tomography. British Journal of Ophthalmology, 2015, 99, 1315-1319.	3.9	34
48	In vivo Retinal Fluorescence Imaging With Curcumin in an Alzheimer Mouse Model. Frontiers in Neuroscience, 2020, 14, 713.	2.8	34
49	Functional Assessment of Cardiac Responses of Adult Zebrafish (Danio rerio) to Acute and Chronic Temperature Change Using High-Resolution Echocardiography. PLoS ONE, 2016, 11, e0145163.	2.5	33
50	Performance and scalability of Fourier domain optical coherence tomography acceleration using graphics processing units. Applied Optics, 2011, 50, 1832.	2.1	31
51	Wavefront sensorless adaptive optics OCT with the DONE algorithm for in vivo human retinal imaging [Invited]. Biomedical Optics Express, 2017, 8, 2261.	2.9	31
52	Effective bidirectional scanning pattern for optical coherence tomography angiography. Biomedical Optics Express, 2018, 9, 2336.	2.9	30
53	Atlas-based shape analysis and classification of retinal optical coherence tomography images using the functional shape (fshape) framework. Medical Image Analysis, 2017, 35, 570-581.	11.6	29
54	Effect of a contact lens on mouse retinal in vivo imaging: Effective focal length changes and monochromatic aberrations. Experimental Eye Research, 2018, 172, 86-93.	2.6	27

#	Article	IF	CITATIONS
55	Construction and use of a zebrafish heart voltage and calcium optical mapping system, with integrated electrocardiogram and programmable electrical stimulation. American Journal of Physiology - Regulatory Integrative and Comparative Physiology, 2015, 308, R755-R768.	1.8	25
56	Coherence-Gated Sensorless Adaptive Optics Multiphoton Retinal Imaging. Scientific Reports, 2016, 6, 32223.	3.3	25
57	Strip-based registration of serially acquired optical coherence tomography angiography. Journal of Biomedical Optics, 2017, 22, 036007.	2.6	25
58	Localization and functional characterization of the p.Asn965Ser (N965S) ABCA4 variant in mice reveal pathogenic mechanisms underlying Stargardt macular degeneration. Human Molecular Genetics, 2018, 27, 295-306.	2.9	24
59	Microvasculature Segmentation and Intercapillary Area Quantification of the Deep Vascular Complex Using Transfer Learning. Translational Vision Science and Technology, 2020, 9, 38.	2.2	24
60	Sensorless adaptive optics multimodal en-face small animal retinal imaging. Biomedical Optics Express, 2019, 10, 252.	2.9	24
61	Drusen in the Peripheral Retina of the Alzheimer's Eye. Current Alzheimer Research, 2018, 15, 743-750.	1.4	24
62	Longitudinal study of retinal degeneration in a rat using spectral domain optical coherence tomography. Optics Express, 2010, 18, 23435.	3.4	23
63	Multiscale sensorless adaptive optics OCT angiography system for in vivo human retinal imaging. Journal of Biomedical Optics, 2017, 22, 1.	2.6	23
64	Exact Surface Registration of Retinal Surfaces From 3-D Optical Coherence Tomography Images. IEEE Transactions on Biomedical Engineering, 2015, 62, 609-617.	4.2	20
65	Retinal optical coherence tomography at 1    μ m with dynamic focus control and axial motion tracking Journal of Biomedical Optics, 2016, 21, 026007.	[•] 2.6	19
66	Scalable, High Performance Fourier Domain Optical Coherence Tomography: Why FPGAs and Not GPGPUs. , 2011, , .		18
67	Aperture phase modulation with adaptive optics: a novel approach for speckle reduction and structure extraction in optical coherence tomography. Biomedical Optics Express, 2019, 10, 552.	2.9	17
68	<title>Prototype laser-activated bimetallic thermal resist for microfabrication</title> ., 2001, , .		16
69	EN FACE OPTICAL COHERENCE TOMOGRAPHY AND OPTICAL COHERENCE TOMOGRAPHY ANGIOGRAPHY OF INNER RETINAL DIMPLES AFTER INTERNAL LIMITING MEMBRANE PEELING FOR FULL-THICKNESS MACULAR HOLES. Retina, 2020, 40, 557-566.	1.7	16
70	Automated identification of cone photoreceptors in adaptive optics optical coherence tomography images using transfer learning. Biomedical Optics Express, 2018, 9, 5353.	2.9	16
71	LF-UNet – A novel anatomical-aware dual-branch cascaded deep neural network for segmentation of retinal layers and fluid from optical coherence tomography images. Computerized Medical Imaging and Graphics, 2021, 94, 101988.	5.8	16
72	Adaptive optics in the mouse eye: wavefront sensing based vs image-guided aberration correction. Biomedical Optics Express, 2019, 10, 4757.	2.9	15

#	Article	IF	CITATIONS
73	Biln: a sensitive bimetallic thermal resist. , 2001, 4345, 557.		14
74	Label-free volumetric imaging of conjunctival collecting lymphatics ex vivo by optical coherence tomography lymphangiography. Journal of Biophotonics, 2018, 11, e201800070.	2.3	14
75	Use of the Retinal Vascular Histology to Validate an Optical Coherence Tomography Angiography Technique. Translational Vision Science and Technology, 2021, 10, 29.	2.2	14
76	Optic Nerve Head Registration Via Hemispherical Surface and Volume Registration. IEEE Transactions on Biomedical Engineering, 2010, 57, 2592-2595.	4.2	13
77	Morphological phenotyping of mouse hearts using optical coherence tomography. Journal of Biomedical Optics, 2014, 19, 1.	2.6	13
78	Wavefront sensor-less adaptive optics using deep reinforcement learning. Biomedical Optics Express, 2021, 12, 5423.	2.9	13
79	Semi-supervised deep learning based 3D analysis of the peripapillary region. Biomedical Optics Express, 2020, 11, 3843.	2.9	13
80	The effect of stiffened diabetic red blood cells on wall shear stress in a reconstructed 3D microaneurysm. Computer Methods in Biomechanics and Biomedical Engineering, 2022, 25, 1691-1709.	1.6	13
81	Clinical explainable differential diagnosis of polypoidal choroidal vasculopathy and age-related macular degeneration using deep learning. Computers in Biology and Medicine, 2022, 143, 105319.	7.0	13
82	Investigation of the Peripapillary Choriocapillaris in Normal Tension Glaucoma, Primary Open-angle Glaucoma, and Control Eyes. Journal of Glaucoma, 2021, 30, 682-689.	1.6	12
83	Bi/In bimetallic thermal resists for microfabrication, photomasks, and micromachining applications. , 2002, 4690, 465.		11
84	Rapid radial optical coherence tomography image acquisition. Journal of Biomedical Optics, 2013, 18, 036004.	2.6	11
85	The route of administration influences the therapeutic index of an anti-proNGF neutralizing mAb for experimental treatment of Diabetic Retinopathy. PLoS ONE, 2018, 13, e0199079.	2.5	11
86	Visible light sensorless adaptive optics for retinal structure and fluorescence imaging. Optics Letters, 2018, 43, 5162.	3.3	11
87	Bimetallic thermal activated films for microfabrication, photomasks, and data storage. , 2002, 4637, 330.		10
88	Comparison of the Clinical Disc Margin Seen in Stereo Disc Photographs With Neural Canal Opening Seen in Optical Coherence Tomography Images. Journal of Glaucoma, 2014, 23, 360-367.	1.6	10
89	Subconjunctival Delivery of p75 ^{NTR} Antagonists Reduces the Inflammatory, Vascular, and Neurodegenerative Pathologies of Diabetic Retinopathy. , 2017, 58, 2852.		10
90	Non-invasive cellular-resolution retinal imaging with two-photon excited fluorescence. Biomedical Optics Express, 2019, 10, 4859.	2.9	10

#	Article	IF	CITATIONS
91	Full-field swept-source phase microscopy. , 2006, , .		9
92	Automatic detection of subretinal fluid and sub-retinal pigment epithelium fluid in optical coherence tomography images. , 2013, 2013, 7388-91.		9
93	Quantitative Evaluation of Transform Domains for Compressive Sampling-Based Recovery of Sparsely Sampled Volumetric OCT Images. IEEE Transactions on Biomedical Engineering, 2013, 60, 470-478.	4.2	9
94	In retinitis pigmentosa TrkC.T1-dependent vectorial Erk activity upregulates glial TNF-α, causing selective neuronal death. Cell Death and Disease, 2017, 8, 3222.	6.3	9
95	Optimizing 3D retinal vasculature imaging in diabetic retinopathy using registration and averaging of OCT-A. Biomedical Optics Express, 2021, 12, 553.	2.9	9
96	Quantitative multi-contrast in vivo mouse imaging with polarization diversity optical coherence tomography and angiography. Biomedical Optics Express, 2020, 11, 6945.	2.9	9
97	Numerical calibration method for a multiple spectrometer-based OCT system. Biomedical Optics Express, 2022, 13, 1685.	2.9	9
98	Fourier Domain Optical Coherence Tomography as a Noninvasive Means for In Vivo Detection of Retinal Degeneration in Xenopus laevis Tadpoles. , 2010, 51, 1066.		8
99	Bimodal in vivo imaging provides early assessment of stem-cell-based photoreceptor engraftment. Eye, 2015, 29, 681-690.	2.1	8
100	Evaluating Signs of Microangiopathy Secondary to Diabetes in Different Areas of the Retina with Swept Source OCTA. , 2020, 61, 8.		8
101	Phase-corrected buffer averaging for enhanced OCT angiography using FDML laser. Optics Letters, 2021, 46, 3833.	3.3	8
102	Substantially thinner internal granular layer and reduced molecular layer surface in the cerebellar cortex of the Tc1 mouse model of down syndrome – a comprehensive morphometric analysis with active staining contrast-enhanced MRI. NeuroImage, 2020, 223, 117271.	4.2	7
103	Pupil segmentation adaptive optics for invivo mouse retinal fluorescence imaging. Optics Letters, 2017, 42, 1365.	3.3	7
104	Age and Glaucoma-Related Characteristics in Retinal Nerve Fiber Layer and Choroid: Localized Morphometrics and Visualization Using Functional Shapes Registration. Frontiers in Neuroscience, 2017, 11, 381.	2.8	6
105	Transfer Learning with U-Net type model for Automatic Segmentation of Three Retinal Layers In Optical Coherence Tomography Images. , 2019, , .		5
106	Automatic Cycle Averaging for Denoising Approximately Periodic Spatiotemporal Signals. IEEE Transactions on Medical Imaging, 2014, 33, 1749-1759.	8.9	4
107	Quantifying Variability in Longitudinal Peripapillary RNFL and Choroidal Layer Thickness Using Surface Based Registration of OCT Images. Translational Vision Science and Technology, 2017, 6, 11.	2.2	4
108	Longitudinal Analysis of Bruch Membrane Opening Morphometry in Myopic Glaucoma. Journal of Glaucoma, 2019, 28, 889-895.	1.6	4

#	Article	IF	CITATIONS
109	Therapeutic Neuroprotection by an Engineered Neurotrophin that Selectively Activates Tropomyosin Receptor Kinase (Trk) Family Neurotrophin Receptors but Not the p75 Neurotrophin Receptor. Molecular Pharmacology, 2021, 100, 491-501.	2.3	4
110	Acute Macular Neuroretinopathy Associated With Chikungunya Fever. Ophthalmic Surgery Lasers and Imaging Retina, 2016, 47, 596-599.	0.7	4
111	Exposure time dependence of image quality in high-speed retinal in vivo Fourier domain OCT. , 2005, , .		3
112	Molecular contrast optical coherence tomography: SNR comparison of techniques and introduction of ground state recovery pump-probe OCT. , 2005, , .		3
113	ADAPTIVE OPTICS OPTICAL COHERENCE TOMOGRAPHY IN A CASE OF ACUTE ZONAL OCCULT OUTER RETINOPATHY. Retinal Cases and Brief Reports, 2020, Publish Ahead of Print, .	0.6	3
114	Validation of glaucoma-like features in the rat episcleral vein cauterization model. Chinese Medical Journal, 2014, 127, 359-64.	2.3	3
115	Endoscopic optical coherence tomography of the retina at 1310 nm using paired-angle rotating scanning. , 2007, , .		2
116	Spectral domain fluorescence coherence phase microscopy. Applied Optics, 2011, 50, 1798.	2.1	2
117	Morphometry of the myopic optic nerve head using FDOCT. , 2011, , .		2
118	Adaptive optics: optical coherence tomography system for in-vivo imaging of the mouse retina. Proceedings of SPIE, 2012, , .	0.8	2
119	GPU accelerated OCT processing at megahertz axial scan rate and high resolution video rate volumetric rendering. Proceedings of SPIE, 2013, , .	0.8	2
120	Segmentation of the macular choroid in OCT images acquired at 830nm and 1060nm. , 2013, , .		2
121	On identification of sinoatrial node in zebrafish heart based on functional time series from optical mapping. , 2013, 2013, 6518-21.		2
122	Multispectral scanning laser ophthalmoscopy combined with optical coherence tomography for simultaneous <i>in vivo</i> mouse retinal imaging. Proceedings of SPIE, 2015, , .	0.8	2
123	Enhancing the visualization of human retina vascular networks by Graphics Processing Unit accelerated speckle variance OCT and graph cut retinal layer segmentation. Proceedings of SPIE, 2015, ,	0.8	2
124	Anterior Segment Optical Coherence Tomography for Targeted Transconjunctival Suture Placement in Overfiltering Trabeculectomy Blebs. Journal of Glaucoma, 2017, 26, 486-490.	1.6	2
125	Multiple instance learning for age-related macular degeneration diagnosis in optical coherence tomography images. , 2017, , .		2
126	Multi-scale and -contrast sensorless adaptive optics optical coherence tomography. Quantitative Imaging in Medicine and Surgery, 2019, 9, 757-768.	2.0	2

#	Article	IF	CITATIONS
127	Pseudoâ€realâ€time retinal layer segmentation for highâ€resolution adaptive optics optical coherence tomography. Journal of Biophotonics, 2020, 13, e202000042.	2.3	2
128	Quantitative Optical Coherence Tomography Angiography in Patients with Moyamoya Vasculopathy: A Pilot Study. Neuro-Ophthalmology, 2021, 45, 386-390.	1.0	2
129	Effect of optical coherence tomography and angiography sampling rate towards diabetic retinopathy severity classification. Biomedical Optics Express, 2021, 12, 6660.	2.9	2
130	INVESTIGATING MICROANGIOPATHY USING SWEPT-SOURCE OPTICAL COHERENCE TOMOGRAPHY ANGIOGRAPHY IN PATIENTS WITH SUSAC SYNDROME. Retina, 2021, 41, 2172-2178.	1.7	2
131	Investigation of the effect of directional (off-axis) illumination on the reflectivity of retina layers in mice using swept-source optical coherence tomography. , 2018, , .		2
132	SNR enhancement through phase dependent signal reconstruction algorithms for phase separated interferometric signals. Optics Express, 2007, 15, 10103.	3.4	1
133	Imaging retinal degeneration in mice by combining Fourier domain optical coherence tomography and fluorescent scanning laser ophthalmoscopy. Proceedings of SPIE, 2009, , .	0.8	1
134	AO-OCT for in vivo mouse retinal imaging: Application of adaptive lens in wavefornt sensorless aberration correction. , 2014, , .		1
135	Sensorless adaptive optics optical coherence tomography for two photon excited fluorescence mouse retinal imaging. , 2019, , .		1
136	Real time volumetric region of interest tracking for sensorless adaptive optics retinal imaging. , 2019, , .		1
137	Long-term assessment of internal limiting membrane peeling for full-thickness macular hole using en face adaptive optics and conventional optical coherence tomography. Canadian Journal of Ophthalmology, 2021, , .	0.7	1
138	Effective Scanning Protocol for Optical Coherence Tomography and Angiography using a 1.6 MHz Fourier Domain Mode-Locked Laser Source. , 2021, , .		1
139	Progress on Bimodal Adaptive Optics OCT and Two-Photon Imaging. , 2021, , .		1
140	Real-time retinal layer segmentation of adaptive optics optical coherence tomography angiography with deep learning. , 2020, , .		1
141	Progress on Multimodal Adaptive Optics OCT and Multiphoton Imaging. , 2020, , .		1
142	Instantaneous complex spectral domain OCT using 3x3 fiber couplers. , 2004, , .		0
143	Rapid volumetric imaging of the human retina in vivo using a low-cost spectral domain optical coherence tomography system. , 2005, , .		Ο
144	Spectrometer based Fourier domain optical coherence tomography of the mouse retina. , 2008, , .		0

#	Article	IF	CITATIONS
145	A 2-DOF embeddable angular displacement sensor based on optical fiber bending loss. , 2009, , .		Ο
146	Evaluating the scalability of high-performance, Fourier-Domain Optical Coherence Tomography on GPGPUs and FPGAs. , 2011, , .		0
147	Ultrahigh-speed ultrahigh-resolution adaptive optics: optical coherence tomography system for in-vivo small animal retinal imaging. Proceedings of SPIE, 2013, , .	0.8	Ο
148	Depth Resolved Aberration Correction with Wavefront Sensorless Adaptive Optics Optical Coherence Tomography. , 2015, , .		0
149	Comparison of a novel adaptive lens with deformable mirrors and its application in high-resolution in-vivo OCT imaging. , 2015, , .		0
150	Automatic optimization high-speed high-resolution OCT retinal imaging at $1\hat{l}$ 4m. , 2015, , .		0
151	Progress on developing wavefront sensorless adaptive optics optical coherence tomography for in vivo retinal imaging in mice. Proceedings of SPIE, 2015, , .	0.8	0
152	Two photon imaging of mouse retina with sensorless adaptive optics. , 2016, , .		0
153	Wavefront sensorless approaches to adaptive optics for in vivo fluorescence imaging of mouse retina. , 2016, , .		0
154	Adaptive optics OCT using 1060nm swept source and dual deformable lenses for human retinal imaging. Proceedings of SPIE, 2016, , .	0.8	0
155	Progress on wavefront sensorless adaptive optics. , 2017, , .		Ο
156	Spectral domain second harmonic optical coherence tomography. , 2005, , .		0
157	Quadrature Projection Complex Conjugate Resolved Fourier Domain Optical Coherence Tomography For Real Time Full Depth Imaging. , 2006, , .		Ο
158	1/f Noise in Spectrometer-Based Optical Coherence Tomography. , 2008, , .		0
159	Imaging of Ocular Angle Structures with Fourier Domain Optical Coherence Tomography. Journal of Current Glaucoma Practice, 2013, 7, 85-87.	0.5	Ο
160	Wavefront Sensorless Adaptive Optics for Ophthalmic Imaging. , 2015, , .		0
161	Adaptive optics with combined optical coherence tomography and scanning laser ophthalmoscopy for in vivo mouse retina imaging. , 2018, , .		0
162	Machine learning for optical coherence tomography angiography. , 2019, , .		0

#	Article	IF	CITATIONS
163	Multi-Contrast OCTA for Small Animal Imaging. , 2020, , .		0
164	Effect of Optical Coherence Tomography Acquisition Sampling Rate Towards Diabetic Retinopathy Severity Classification. , 2021, , .		0
165	Progress on multimodal retinal imaging via OCT and two photon excited fluorescence. , 2021, , .		0